

Cite this: *Dalton Trans.*, 2014, **43**, 15138

## Silver nanoparticles supported on passivated silica: preparation and catalytic performance in alkyne semi-hydrogenation†

Emma Oakton,<sup>a</sup> Gianvito Vilé,<sup>b</sup> Daniel S. Levine,<sup>c,d</sup> Eva Zocher,<sup>a,c,e</sup> David Baudouin,<sup>a</sup> Javier Pérez-Ramírez\*<sup>b</sup> and Christophe Copéret\*<sup>a,c</sup>

Herein, we report the preparation of small and narrowly distributed ( $2.1 \pm 0.5$  nm) Ag nanoparticles supported on passivated silica, where the surface OH groups are replaced by OSiMe<sub>3</sub> functionalities. This synthetic method involves the grafting of silver(I) bis(trimethylsilyl)amide ([AgN(SiMe<sub>3</sub>)<sub>2</sub>]<sub>2</sub>) on silica partially dehydroxylated at 700 °C, followed by a thermal treatment of the grafted complex under H<sub>2</sub>. The catalytic performance of this material was investigated in the semi-hydrogenation of propyne and 1-hexyne and compared with that of  $2.0 \pm 0.3$  nm Ag nanoparticles supported on silica. Whilst surface passivation slightly decreases the activity in both reactions (by a factor 2–3), probably as a result of the decreased alkyne adsorption properties or the presence of less accessible active sites on the passivated support, the Ag<sub>NP</sub>@SiO<sub>2</sub> catalysts demonstrate a remarkable selectivity for the production of alkenes.

Received 3rd May 2014,  
Accepted 29th July 2014  
DOI: 10.1039/c4dt01320d

www.rsc.org/dalton

## Introduction

Controlling the size, shape and composition of supported metal nanoparticles has been a vibrant field of research for more than 100 years,<sup>1,2</sup> in view of their critical impact on many industrial processes.<sup>2,3</sup> An important aspect of these supported catalysts is the interface between the nanoparticles and the support.<sup>4–7</sup> In fact, adjusting adsorption properties whilst keeping the same support can affect both the activity and selectivity of a catalyst by altering the active sites and/or their surroundings. For instance, it has been shown that the replacement of surface hydroxyl groups by trimethylsilyl functionalities (surface passivation) has a positive effect on the

catalytic performances of single-site catalysts,<sup>8</sup> e.g. Ti-based epoxidation catalysts,<sup>9–12</sup> Ta-based silica-supported epoxidation catalysts<sup>13</sup> and Re-based alumina-supported metathesis catalysts.<sup>14</sup> Moreover, passivation effects have also been observed for supported nanoparticle catalysts, such as Au nanoparticles supported on passivated silica, which outperform the alternative titania-supported gold catalyst in the aerobic epoxidation of stilbene.<sup>15</sup> In addition, surface passivation can provide mechanistic clues to the role of the OH groups of the support in metal catalysis. In fact, Au nanoparticles supported on passivated silica require H<sub>2</sub> to oxidise CO with O<sub>2</sub>, while this reaction takes place with or without H<sub>2</sub> on Au nanoparticles supported on hydroxylated silica, suggesting that the proton of the OH group can provide surface Au–H hydrides.<sup>16</sup>

The catalytic activity of Ag nanoparticles towards a variety of hydrogenation reactions has been shown previously.<sup>17–20</sup> We recently investigated the gas-phase semi-hydrogenation of propyne, an industrially relevant reaction for the purification of olefin streams,<sup>21</sup> using silica-supported Ag nanoparticles.<sup>22</sup> Whilst various alkyne semi-hydrogenation catalysts have been developed,<sup>18,23–27</sup> noteworthy was the very high alkene selectivity (*ca.* 90%) at a high degree of alkyne conversion for our Ag catalyst.<sup>22</sup> This study<sup>22</sup> revealed that the selective character of Ag stems from the unique mechanism, which occurs on Ag surfaces. Namely, in contrast to most metals for which hydrogenation takes place *via* the classical Horiuti–Polanyi mechanism (dissociation of H<sub>2</sub> on the metal surface followed by sequential H addition), the key elementary step for the Ag cata-

<sup>a</sup>Laboratory of Inorganic Chemistry, Department of Chemistry and Applied Biosciences, ETH Zürich, Vladimir-Prelog Weg 2, Zürich, Switzerland.  
E-mail: ccoperet@inorg.chem.ethz.ch

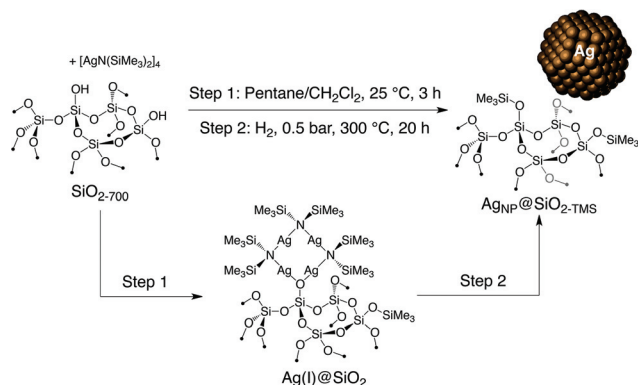
<sup>b</sup>Institute for Chemical and Bioengineering, Department of Chemistry and Applied Biosciences, ETH Zürich, Vladimir-Prelog Weg 1, Zürich, Switzerland.  
E-mail: jpr@chem.ethz.ch

<sup>c</sup>Université de Lyon, Institut de Chimie de Lyon, UMR C2P2 CNRS-UCBL-ESCEP Lyon, 43 Bd. du 11 Novembre 1918, 69616 Villeurbanne, France

<sup>d</sup>Department of Chemistry, 419 Latimer Hall, University of California, Berkeley, CA 94720-1460, USA

<sup>e</sup>Wacker Chemie AG, Hanns-Seidel Platz 4, 81737 München, Germany

† Electronic supplementary information (ESI) available: <sup>1</sup>H and <sup>13</sup>C MAS NMR spectra of Ag(I)@SiO<sub>2</sub>; Activity and selectivity of Ag<sub>NP</sub>@SiO<sub>2</sub>-TMS and Ag<sub>NP</sub>@SiO<sub>2</sub>-OH at 75% conversion for the semi-hydrogenation and propyne; TEM images of Ag<sub>NP</sub>@SiO<sub>2</sub>-TMS and Ag<sub>NP</sub>@SiO<sub>2</sub>-OH after semi-hydrogenation of propyne; H<sub>2</sub> and propyne adsorption on Ag<sub>NP</sub>@SiO<sub>2</sub>-TMS and Ag<sub>NP</sub>@SiO<sub>2</sub>-OH. See DOI: 10.1039/c4dt01320d



Scheme 1 Preparation of  $\text{Ag}_{\text{NP}}\text{@SiO}_2\text{-TMS}$ .

lysed reaction is the direct activation of  $\text{H}_2$  on the chemisorbed alkyne, probably at B5 step sites.<sup>22,28,29</sup> One of the major problems in the catalytic semi-hydrogenation of alkynes is the production of green-oil, an oligomeric by-product, which can cause catalyst deactivation and equipment blockage.<sup>21,30</sup> Interestingly, it has been shown for the related Pd-based supported alkyne hydrogenation catalysts that the support itself has a large influence over the formation of such by-products.<sup>30</sup> With this in mind, and in view of the dramatic effect of surface passivation on the catalytic activity of silica-supported Au nanoparticles,<sup>15</sup> we have investigated the effect of surface passivation on the activity and selectivity of silica-supported Ag nanoparticles in the semi-hydrogenation of alkynes. Particularly, we report the catalytic performance in the semi-hydrogenation of propyne and 1-hexyne on Ag nanoparticles supported on passivated silica prepared *via* the controlled reaction of  $[\text{AgN}(\text{SiMe}_3)_2]_4$ <sup>31,32</sup> with  $\text{SiO}_2\text{-700}$  and thermal treatment under  $\text{H}_2$  (Scheme 1).

## Results & discussion

The reaction of excess of  $[\text{AgN}(\text{SiMe}_3)_2]_4$  (2 equiv. Ag per surface silanol) in a 1:1 pentane–dichloromethane mixture with  $\text{SiO}_2\text{-700}$  led to a white solid,  $\text{Ag}(\text{I})\text{@SiO}_2$ , which was characterised by elemental analysis, IR spectroscopy and solid-state NMR spectroscopy. During this step, all surface silanols are consumed as evidenced by the disappearance of the Si–O–H band, at  $3745\text{ cm}^{-1}$ , in the IR spectrum (Fig. 1a) accompanied by the appearance of C–H bands at  $2897$ ,  $2952$  and  $1400\text{ cm}^{-1}$ . These data are consistent with the chemical grafting of  $[\text{AgN}(\text{SiMe}_3)_2]_4$  on the silanol groups of the silica surface.  $^1\text{H}$  magic angle spinning (MAS) solid-state NMR confirms the total consumption of silanols as evidenced by the absence of a Si–O–H peak at 1.8 ppm (Fig. S1†), while a single proton environment at 0 ppm indicates the presence of  $\text{SiMe}_3$  surface ligands. Furthermore, in the  $^{13}\text{C}$  High-Power DECOupled (HPDEC) MAS NMR spectrum two distinguishable  $\text{SiMe}_3$  groups are observed at 0 and 6.5 ppm, indicating that there are two types of trimethylsilyl groups present associated with  $\text{O}-\text{Si}(\text{CH}_3)_3$  and

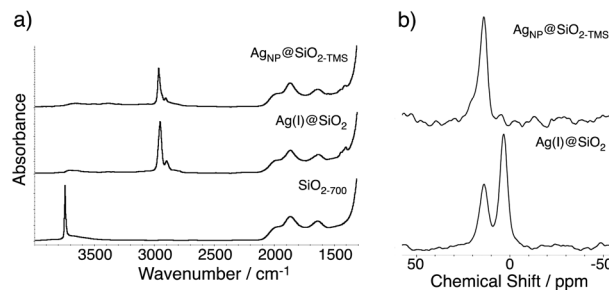


Fig. 1 (a) IR spectrum of  $\text{SiO}_2\text{-700}$ ,  $\text{Ag}(\text{I})\text{@SiO}_2$  and  $\text{Ag}_{\text{NP}}\text{@SiO}_2\text{-TMS}$  and (b)  $^{29}\text{Si}$  CPMAS (5 kHz, 400 MHz,  $n_s = 51200$ ) NMR of  $\text{Ag}(\text{I})\text{@SiO}_2$  and  $\text{Ag}_{\text{NP}}\text{@SiO}_2\text{-TMS}$ .

$\text{N}-(\text{Si}(\text{CH}_3)_3)_2$  functionalities respectively (Fig. S2†).<sup>33,34</sup> The relative intensity of these peaks gives a  $\text{O}-\text{Si}(\text{CH}_3)_3 : \text{N}-\text{Si}(\text{CH}_3)_3$  ratio of *ca.* 1 : 4. This assignment is corroborated by  $^{29}\text{Si}$  cross-polarisation (CP) MAS NMR spectroscopy, with the observation of two peaks at 3 and 14 ppm corresponding to  $\text{Ag}-\text{N}(\text{SiMe}_3)_2$  and  $\text{O}-\text{SiMe}_3$  surface species respectively (Fig. 1b). It is noteworthy that this solid contains 4.4 wt% of Ag, corresponding to  $1.2\text{ Ag nm}^{-2}$  ( $1.6\text{ Ag per SiOH}$ ), which exceeds the initial OH density. In addition, N elemental analysis results of 0.69 wt% suggests that the ratio of Ag:N is nearly constant (1:1.2). Furthermore, in view of the presence of  $\text{O}-\text{Si}(\text{CH}_3)_3$ , which results from the subsequent reaction of  $\text{HN}(\text{Si}(\text{CH}_3)_3)_2$ ,<sup>35</sup> released upon the reaction of the surface silanol with  $[\text{AgN}(\text{SiMe}_3)_2]_4$ , there is a clear indication for the formation of multinuclear Ag species. The ratio of  $\text{OSiMe}_3$ -to- $\text{N}(\text{SiMe}_3)_2$  of 1 : 3.7 and the presence of  $1.2\text{ Ag nm}^{-2}$  determined by elemental analysis are consistent with the formation of  $\text{OSiMe}_3$  ( $0.5\text{ per nm}^2$ ) and Ag species present as tetranuclear species as in the molecular precursor. The proposed surface species, noted as  $\text{Ag}(\text{I})\text{@SiO}_2$  in Scheme 1, is grafted through one O–Ag linkage ( $0.3\text{ per nm}^2$ ). In fact, the formation of multinuclear species was previously observed in the grafting of tetra-nuclear  $[\text{Cu}(\text{OtBu})_4]$  and  $[\text{Cu}(\text{OSi}(\text{OtBu})_3)_4]$  species and assigned to linearly arranged Cu at the surface.<sup>36</sup>

Treatment of  $\text{Ag}(\text{I})\text{@SiO}_2$  with  $\text{H}_2$  (0.5 bar) at  $300\text{ °C}$  for 20 h yields a homogeneous dark orange solid. Transmission electron microscopy of the sample exposed to air shows the presence of nanoparticles having an average diameter of 2.1 nm with narrow size distribution of 0.5 nm (Fig. 2), which

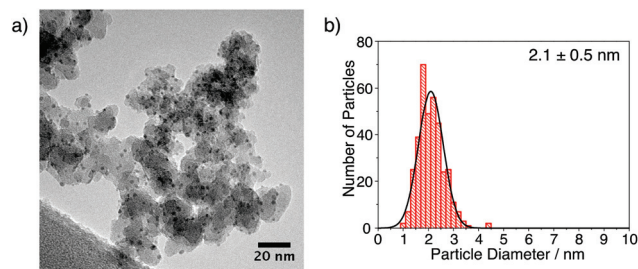


Fig. 2 (a) TEM image and (b) particle size distribution of  $\text{Ag}_{\text{NP}}\text{@SiO}_2\text{-TMS}$ .

corresponds to a dispersion of *ca.* 55% assuming that the particles have a cubooctahedral shape.<sup>37</sup> IR spectroscopy of this material, Ag<sub>NP</sub>@SiO<sub>2-TMS</sub>, shows that silanol functionalities are not regenerated upon H<sub>2</sub> treatment (the absence of a peak at 3745 cm<sup>-1</sup>) while the trimethylsilyl groups remain, as evidenced by the  $\nu_{C-H}$  bands at 2964 and 2906 cm<sup>-1</sup>. Note however that the presence of new bands at 3300–3500 cm<sup>-1</sup> are attributed to N–H vibrations (Fig. S3†), resulting from the hydrogenolysis of the AgN(SiMe<sub>3</sub>)<sub>2</sub> species and the probable incorporation of NH<sub>x</sub> into the silica surface.<sup>38</sup> Additionally, the C–H bands have decreased by comparison with Ag(1)@SiO<sub>2</sub>, suggesting that some of these species have been removed upon H<sub>2</sub> treatment. The <sup>29</sup>Si CPMAS spectrum of Ag<sub>NP</sub>@SiO<sub>2-TMS</sub> displays a single peak at 14 ppm (Fig. 1b), consistent with the sole presence of O–SiMe<sub>3</sub> surface functionalities and indicating that “Ag–N(SiMe<sub>3</sub>)<sub>2</sub>” moieties of Ag(1)@SiO<sub>2</sub> have been fully converted upon H<sub>2</sub> treatment. In view of the formation of Ag-nanoparticles, SiO–Ag bonds are probably cleaved by H<sub>2</sub> to regenerate SiOH and provide Ag(0), which leads to the formation of the nanoparticles. It is likely that the thus-formed SiOH reacts with the released HN(SiMe<sub>3</sub>)<sub>2</sub> leading to a surface covered with OSiMe<sub>3</sub> species and Ag nanoparticles. This process is reminiscent of what has been observed in the formation of nanoparticles from the analogous gold complex.<sup>15</sup>

The catalytic performance of Ag<sub>NP</sub>@SiO<sub>2-TMS</sub> was first evaluated in the semi-hydrogenation of propyne. Fig. 3a depicts the selectivity of Ag<sub>NP</sub>@SiO<sub>2-TMS</sub> towards propene as a function of the conversion of propyne. Ag<sub>NP</sub>@SiO<sub>2-TMS</sub> maintains a high

alkene selectivity (87–93%) over a broad range of propyne conversions (10–100%). Also noteworthy is the constant and low selectivity of this catalyst towards propane and oligomers as previously observed for Ag nanoparticles supported on hydroxylated silica.<sup>22</sup> To determine the effect of surface passivation on this reaction, these results were compared with 1 wt% Ag 2.0 ± 0.3 nm Ag nanoparticles supported on silica (57% dispersion), having surface silanols.<sup>22</sup> It is noteworthy that preparation of this material, Ag<sub>NP</sub>@SiO<sub>2-OH</sub>, with a higher Ag wt% loading resulted in considerably larger Ag particles.<sup>22</sup> At 20% propyne conversion, the propene selectivity of both catalysts is high; Ag<sub>NP</sub>@SiO<sub>2-TMS</sub> shows an improvement with a value of 94% in comparison with 86% for Ag<sub>NP</sub>@SiO<sub>2-OH</sub> (Fig. 3b). However, at 75% propyne conversion, the selectivity of both catalysts is similar (*ca.* 90%, see Fig. S5†) indicating that secondary processes are not affected by the surface functionalities.

In addition, the rate of reaction over Ag<sub>NP</sub>@SiO<sub>2-TMS</sub>, at 20% propyne conversion, is *ca.* 2.5 times lower than that of Ag<sub>NP</sub>@SiO<sub>2-OH</sub> (0.78 mmol<sub>C<sub>3H<sub>6</sub></sub> s<sup>-1</sup> mol<sub>Ag</sub><sup>-1</sup> vs. 2.1 mmol<sub>C<sub>3H<sub>6</sub></sub> s<sup>-1</sup> mol<sub>Ag</sub><sup>-1</sup> respectively), while the activity expressed per gram of the catalyst favours Ag<sub>NP</sub>@SiO<sub>2-TMS</sub> over Ag<sub>NP</sub>@SiO<sub>2-OH</sub> (1.7 mmol<sub>C<sub>3H<sub>6</sub></sub> s<sup>-1</sup> g<sup>-1</sup> vs. 1.1 mmol<sub>C<sub>3H<sub>6</sub></sub> s<sup>-1</sup> g<sup>-1</sup> respectively), because of the higher Ag loading (*ca.* 4 times) in Ag<sub>NP</sub>@SiO<sub>2-TMS</sub>. A similar activity trend was also observed in the three-phase fully selective (>99%) semi-hydrogenation of 1-hexyne (Fig. 3c). This decrease in activity is not due to a difference in particle sizes, which are similar (2.1 ± 0.5 nm for Ag<sub>NP</sub>@SiO<sub>2-TMS</sub> vs. 2.0 ± 0.3 nm for Ag<sub>NP</sub>@SiO<sub>2-OH</sub>) and do not increase during the catalytic tests (Fig. S6†). The lower activity for the semi-hydrogenation of propyne may be due to differences in reactant adsorption, or to the presence of less accessible active sites as a result of surface passivation in Ag<sub>NP</sub>@SiO<sub>2-TMS</sub>. To further elucidate the origin of this difference in activity, the adsorption of H<sub>2</sub> and propyne was measured (Fig. S7 and S8† respectively). Adsorption measurements showed that both catalysts adsorb negligible amounts of H<sub>2</sub> at 290 mbar and 0 °C (0.002 ± 0.003 and 0.005 ± 0.003 mmol<sub>H<sub>2</sub></sub> g<sub>sample</sub><sup>-1</sup> for Ag<sub>NP</sub>@SiO<sub>2-TMS</sub> and Ag<sub>NP</sub>@SiO<sub>2-OH</sub>, respectively, <0.02 H per Ag<sub>surface</sub>). Moreover, propyne adsorption is found to be slightly lower for the passivated catalyst, with 0.90 ± 0.02 vs. 0.96 ± 0.04 mmol<sub>C<sub>3H<sub>4</sub></sub> g<sub>sample</sub><sup>-1</sup> for Ag<sub>NP</sub>@SiO<sub>2-TMS</sub> and Ag<sub>NP</sub>@SiO<sub>2-OH</sub>, respectively. However, this difference is particularly striking when the adsorption is expressed in mmol of adsorbed propyne per mmol surface Ag: 18 mmol<sub>C<sub>3H<sub>4</sub></sub> mmol<sub>Ag</sub><sup>-1</sup> for Ag<sub>NP</sub>@SiO<sub>2-OH</sub> vs. 4 mmol<sub>C<sub>3H<sub>4</sub></sub> mmol<sub>Ag</sub><sup>-1</sup> for Ag<sub>NP</sub>@SiO<sub>2-TMS</sub>. This decrease in propyne adsorption on Ag<sub>NP</sub>@SiO<sub>2-TMS</sub> may be due to the change in support surface functionalisation and/or density effects due to the increased Ag loading on the Ag<sub>NP</sub>@SiO<sub>2-TMS</sub> sample. Since the rate-determining step for the hydrogenation of propyne on Ag nanoparticles is associated with the dissociation of H<sub>2</sub> on adsorbed propyne,<sup>22</sup> the difference in reactivity between the two catalysts could originate from the decreased adsorption of the alkyne on Ag<sub>NP</sub>@SiO<sub>2-TMS</sub>, the higher density of particles or a decreased amount of active sites as a result of passivation of the silica surface.</sub></sub></sub></sub></sub></sub></sub>

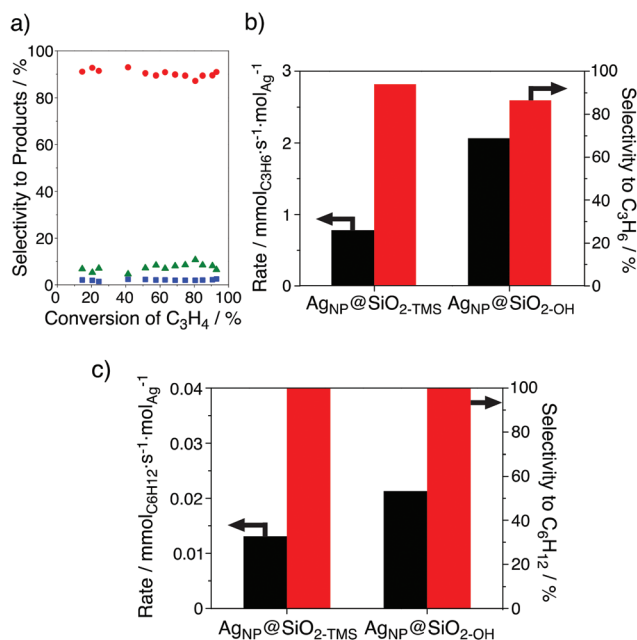


**Fig. 3** (a) Selectivity–conversion relationship for Ag<sub>NP</sub>@SiO<sub>2-TMS</sub> to propene (red circles), propane (blue squares) and oligomers (green triangles). Activity and selectivity of Ag<sub>NP</sub>@SiO<sub>2-TMS</sub> and Ag<sub>NP</sub>@SiO<sub>2-OH</sub> at 20% conversion in (b) the gas-phase hydrogenation of propyne and (c) liquid-phase hydrogenation of 1-hexyne.



## Conclusions

Using surface organometallic chemistry, we have prepared small Ag nanoparticles ( $2.1 \pm 0.5$  nm) supported on passivated silica, through the controlled reaction of the partially dehydroxylated support with silver(i) bistrimethylsilylamide to form well-defined silica-supported Ag(i) bis(trimethylsilyl)amide tetranuclear clusters, as well as surface SiMe<sub>3</sub> groups. These species are then decomposed to form nanoparticles by a controlled H<sub>2</sub> treatment. The small size and narrow distribution of the Ag particles prepared by this route is particularly important considering the high Ag weight loading (4.4 wt%). This catalyst displays good selectivity (*ca.* 90%) in the gas-phase semi-hydrogenation of propyne, even at high propyne conversion, and full selectivity to the alkene in the liquid-phase hydrogenation of 1-hexyne. These results suggest that, in this case, the surface OH functionalities do not take part in the semi-hydrogenation of propyne, as the selectivity towards propene remains remarkably highly independent of support passivation. However, this modification of the support surface results in a decrease in reaction rate (by a factor of *ca.* 2–3), possibly due to a decrease in the number of adsorbed propyne molecules per surface Ag for the Me<sub>3</sub>Si-functionalised support; yet as a result of much higher loading the activity of the catalyst is *ca.* twice higher per gram of catalysts. We are currently further exploring the effect of surface functionalities in controlling the catalytic activity and selectivity of supported metal nanoparticles.

## Experimental

### General

All experiments were conducted under an argon atmosphere using standard Schlenk and glove-box techniques unless otherwise stated. Solvents were dried over an alumina column (MB SPS-800, MBraun), stored over 4 Å molecular sieves and degassed before use. H<sub>2</sub> (99.999%) was purchased from PanGas and propyne (99%) was supplied by Sigma-Aldrich. 1-Hexyne was purchased from Acros Organics (98%). IR measurements were performed using a Bruker Alpha-T FTIR spectrometer inside an argon-filled glove-box. Samples were pressed into a self-supporting disk for acquisition using a manual press. NMR spectroscopy was conducted using a 400 MHz Bruker spectrometer. Elemental analysis was conducted at Pascher Analytical Labor in Germany. TEM images were collected with a Philips CM12 transmission electron microscope.

### Catalyst preparation

**Preparation of [AgN(SiMe<sub>3</sub>)<sub>2</sub>]<sub>4</sub>.** [AgN(SiMe<sub>3</sub>)<sub>2</sub>]<sub>4</sub> was prepared according to a modified literature procedure.<sup>31,39</sup> Equimolar amounts of silver(i) trifluoromethanesulfonate and lithium bis(trimethylsilyl)amide were reacted in Et<sub>2</sub>O at room temperature for 16 h in the absence of light. After extraction with pentane and recrystallisation, silver(i) bis(trimethylsilyl)amide was isolated as colourless crystals in 15% yield. <sup>1</sup>H NMR (300 MHz, CD<sub>2</sub>Cl<sub>2</sub>);  $\delta$  = 0.29 ppm. <sup>1</sup>H MAS (10 kHz, 400 MHz);

$\delta$  = -0.4 ppm. <sup>13</sup>C CPMAS (10 kHz, 400 MHz);  $\delta$  = 8.6 ppm. <sup>29</sup>Si CPMAS (10 kHz, 400 MHz);  $\delta$  = 2.8 ppm.

**Preparation of SiO<sub>2-700</sub>.** Silica partially dehydroxylated at 700 °C (SiO<sub>2-700</sub>) was prepared by calcination of compacted Aerosil Degussa (200 m<sup>2</sup> g<sup>-1</sup>) at 500 °C for 14 h followed by a treatment under vacuum (10<sup>-5</sup> mbar) at 700 °C for 5 h (heating rate of 5 °C min<sup>-1</sup> from 500 to 700 °C): 0.26 mmol<sub>SiOH</sub> g<sup>-1</sup>, 0.8 OH nm<sup>-1</sup>.<sup>40</sup>

**Preparation of Ag(i)@SiO<sub>2</sub>.** SiO<sub>2-700</sub> (0.5 g, 0.13 mmol SiOH, 1 equiv.) was contacted with a 1 : 1 pentane–dichloromethane solution of [AgN(SiMe<sub>3</sub>)<sub>2</sub>]<sub>4</sub> (0.073 g, 0.26 mmol<sub>Ag</sub>, 2 Ag equiv. per SiOH) for 3 h at room temperature in the absence of light. After washing 3 times with fresh solvent and drying under high vacuum a white solid, Ag(i)@SiO<sub>2</sub>, was obtained. IR (disk) = 2897, 2952, 1980, 1863, 1629, 1400 cm<sup>-1</sup>. <sup>1</sup>H MAS (10 kHz, 400 MHz);  $\delta$  = 0 ppm. <sup>13</sup>C CPMAS (10 kHz, 400 MHz);  $\delta$  = 0.0, 6.5 ppm. <sup>29</sup>Si CPMAS (10 kHz, 400 MHz);  $\delta$  = 3 and 14 ppm. Elemental analysis; Ag = 4.4, C = 2.3, H = 0.6 and N = 0.7 wt%.

**Preparation of Ag<sub>NP</sub>@SiO<sub>2-TMS</sub>.** Ag(i)@SiO<sub>2</sub> (0.25 g) was treated with H<sub>2</sub> (500 cm<sup>3</sup>, 0.5 bar, 100 H<sub>2</sub> Ag<sup>-1</sup>) dried over R3-11 G (T5 × 3 mm) BASF catalyst and 4 Å molecular sieves and heated with a rate of 5 °C min<sup>-1</sup> and held at 300 °C for 20 h. After cooling, the H<sub>2</sub> atmosphere was removed using ultra-high vacuum techniques. This treatment yielded a dark orange powder. TEM imaging of the solid showed nanoparticles were present on the support surface with an average diameter of 2.1 ± 0.5 nm. <sup>29</sup>Si CPMAS (10 kHz, 400 MHz);  $\delta$  = 14 ppm. Elemental analysis; Ag = 4.3, C = 1.9, H = 0.5 and N = 0.3 wt%.

**Preparation of Ag<sub>NP</sub>@SiO<sub>2-OH</sub>.** This sample was prepared according to a reported procedure.<sup>22</sup>

### Selective hydrogenation of alkynes

The gas-phase hydrogenation of propyne was carried out in a continuous-flow fixed-bed micro-reactor (12 mm i.d.) equipped with an on-line gas chromatograph (Agilent GC7890A), in the absence of internal and external mass transfer limitations (Fig. S4†).<sup>22</sup> Unless otherwise stated, the reactions were performed with 0.2 g of catalyst (particle size = 0.2–0.4 mm), at  $T = 200$  °C,  $P = 1$  bar, H<sub>2</sub>/C<sub>3</sub>H<sub>4</sub> = 25. The contact time,  $\tau$ , was varied between 0.01 and 1 s when assessing the influence of conversion on product distribution and was kept at a value of 0.07 s (alkyne conversion = 20%) when comparing the performance of the different catalysts. The three-phase hydrogenation of 1-hexyne was carried out in a flooded-bed micro-reactor.<sup>41</sup> The reactant solution contained 1 vol% of 1-hexyne (Acros Organics, 98%), 1 vol% of benzene (Sigma-Aldrich, >99.5%) as the internal standard, and 98 vol% of toluene (Acros Organics, 99.9%) as the solvent. The hydrogenation was conducted with 0.2 g of catalyst, at  $T = 313$  K,  $P = 60$  bar,  $F(\text{H}_2) = 60$  cm<sup>3</sup> min<sup>-1</sup>, and  $F(\text{liquid}) = 0.3$  cm<sup>3</sup> min<sup>-1</sup>. The liquid at the reactor outlet was analysed offline with a gas chromatograph (HP 6890) equipped with a HP-5 capillary column and a flame ionization detector. In all cases, the conversion of the alkyne was determined as the amount of reacted alkyne divided by the amount of alkyne at the reactor inlet. The selectivity to the alkene/alkane was calculated as the quantity of alkene/alkane formed divided by the

amount of converted alkyne. The selectivity to oligomers was determined as  $S_{\text{oligomers}} = 100 - S_{\text{alkene}} - S_{\text{alkane}}$ .

### H<sub>2</sub> and propyne adsorption measurements

Adsorption measurements were conducted using a BELSORP-Max instrument from BEL Japan Inc. Around 0.1 g of each catalyst was pre-treated under flowing H<sub>2</sub> at 200 °C with a heating ramp of 5 °C min<sup>-1</sup> for 30 min, followed by evacuation for 3 h at the same temperature. Adsorption measurements were performed using hydrogen and propyne at 0 °C. Langmuir isotherms, non-dissociative, were fitted to the experimental results for propyne adsorption leading to the amount of gas adsorbed per surface metal. In view of the low amount of H<sub>2</sub> adsorbed on both catalysts, it was not possible to fit dissociative Langmuir isotherms and therefore the results reported here correspond to the amount of H<sub>2</sub> adsorbed at 290 mbar.

### Acknowledgements

The authors would like to thank ETH Zürich for financial support. In addition DSL thanks the MIT – France foundation for sponsoring his summer internship in C2P2. We are also grateful to ScopeM for the use of their microscopy facilities and Karol Furman for assistance with adsorption measurements.

### Notes and references

- R. Schlögl and S. B. A. Hamid, *Angew. Chem., Int. Ed.*, 2004, **43**, 1628–1637.
- B. Coq and F. Figueras, *Coord. Chem. Rev.*, 1998, **178–180**, 1753–1783.
- A. T. Bell, *Science*, 2003, **299**, 1688–1691.
- B. R. Cuenya, *Thin Solid Films*, 2010, **518**, 3127–3150.
- X. Wang, P. Sonström, D. Arndt, J. Stöver, V. Zielasek, H. Borchert, K. Thiel, K. Al-Shamery and M. Bäumer, *J. Catal.*, 2011, **278**, 143–152.
- P. Ganesh, P. R. C. Kent and G. M. Veith, *J. Phys. Chem. Lett.*, 2011, **2**, 2918–2924.
- S. J. Tauster, *Acc. Chem. Res.*, 1987, **20**, 389–394.
- C. Copéret, M. Chabanas, R. P. Saint-Arroman and J.-M. Basset, *Angew. Chem., Int. Ed.*, 2003, **42**, 156–181.
- T. Tatsumi, K. A. Koyano and N. Igarashi, *Chem. Commun.*, 1998, 325–326.
- P. J. Cordeiro and T. D. Tilley, *ACS Catal.*, 2011, **1**, 455–467.
- S. A. Holmes, F. Quignard, A. Choplin, R. Teissier and J. Kervennal, *J. Catal.*, 1998, **176**, 182–191.
- R. L. Brutchey, D. A. Ruddy, L. K. Andersen and T. D. Tilley, *Langmuir*, 2005, **21**, 9576–9583.
- P. J. Cordeiro and T. D. Tilley, *Langmuir*, 2011, **27**, 6295–6304.
- A. Salameh, A. Baudouin, J.-M. Basset and C. Copéret, *Angew. Chem., Int. Ed.*, 2008, **47**, 2117–2120.
- D. Gajan, K. Guillois, P. Delichère, J.-M. Basset, J.-P. Candy, V. Caps, C. Copéret, A. Lesage and L. Emsley, *J. Am. Chem. Soc.*, 2009, **131**, 14667–14669.
- M. Conte, H. Miyamura, S. Kobayashi and V. Chechik, *J. Am. Chem. Soc.*, 2009, 7189–7196.
- P. Claus and H. Hofmeister, *J. Phys. Chem. B*, 1999, **103**, 2766–2775.
- A. Sárkány and Z. Révay, *Appl. Catal., A*, 2003, **243**, 347–355.
- M. Steffan, A. Jakob, P. Claus and H. Lang, *Catal. Commun.*, 2009, **10**, 437–441.
- K. H. Lim, A. B. Mohammad, I. V. Yudanov, K. M. Neyman, M. Bron, P. Claus and N. Rösch, *J. Phys. Chem. C*, 2009, **113**, 13231–13240.
- M. L. Derrien, *Catalytic Hydrogenation*, Elsevier, Amsterdam, 1986.
- G. Vilé, D. Baudouin, I. N. Remediakis, C. Copéret, N. López and J. Pérez-Ramírez, *ChemCatChem*, 2013, **5**, 3750–3759.
- M. Crespo-Quesada, F. Cardenas-Lizana, A.-L. Dessimoz and L. Kiwi-Minsker, *ACS Catal.*, 2012, **2**, 1773–1786.
- W. Long, N. A. Brunelli, S. A. Didas, E. W. Ping and C. W. Jones, *ACS Catal.*, 2013, **3**, 1700–1708.
- B. Bridier, N. López and J. Pérez-Ramírez, *J. Catal.*, 2010, **269**, 80–92.
- R. A. Koeppel, J. T. Wehrli, M. S. Wainwright, D. L. Trimm and N. W. Cant, *Appl. Catal., A*, 1994, **120**, 163–177.
- M. Yan, T. Jin, Y. Ishikawa, T. Minato, T. Fujita, L.-Y. Chen, M. Bao, N. Asao, M.-W. Chen and Y. Yamamoto, *J. Am. Chem. Soc.*, 2012, **134**, 17536–17542.
- R. V. Hardeveld and A. V. Montfoort, *Surf. Sci.*, 1966, **4**, 396–430.
- J. Gavnholt and J. Schiøtz, *Phys. Rev. B: Condens. Matter*, 2008, **77**, 035404.
- M. Ruta, N. Semagina and L. Kiwi-Minsker, *J. Phys. Chem. C*, 2008, **112**, 13635–13641.
- P. B. Hitchcock, M. F. Lappert and L. J. M. Pierssens, *Chem. Commun.*, 1996, 1189–1190.
- Y. Liang and R. Anwender, *Dalton Trans.*, 2013, **42**, 12521–12545.
- G. Lapadula, A. Bourdolle, F. Allouche, M. P. Conley, I. D. Rosal, L. Maron, W. W. Lukens, Y. Guyot, C. Andraud, S. Brasselet, C. Copéret, O. Maury and R. A. Andersen, *Chem. Mater.*, 2014, **26**, 1062–1073.
- D. Gajan, D. Levine, E. Zocher, C. Copéret, A. Lesage and L. Emsley, *Chem. Sci.*, 2011, **2**, 926–931.
- R. Anwender, I. Nagl, M. Widenmeyer, G. Engelhardt, O. Groeger, C. Palm and T. Roser, *J. Phys. Chem. B*, 2000, **104**, 3532–3544.
- K. L. Fajdala, I. J. Drake, A. T. Bell and T. D. Tilley, *J. Am. Chem. Soc.*, 2004, **126**, 10864–10866.
- R. E. Benfield, *J. Chem. Soc., Faraday Trans.*, 1992, **88**, 1107–1110.
- T. Asefa, M. Kruk, N. Coombs, H. Grondy, M. J. MacLachlan, M. Jaroniec and G. A. Ozin, *J. Am. Chem. Soc.*, 2003, **125**, 11662–11673.
- Y. Yamashita, T. Imaizumi, X.-X. Guo and S. Kobayashi, *Chem. – Asian J.*, 2011, **6**, 2550–2559.
- L. T. Zhuravlev, in *Colloidal Silica: Fundamentals and Applications*, Crc Press Taylor Francis Group, Boca Raton, 2006.
- G. Vilé, N. Almora-Barrios, S. Mitchell, N. López and J. Pérez-Ramírez, *Chem. – Eur. J.*, 2014, **20**, 5926–5937.